Experimental Investigation on Material Properties due to Simulating Space Environments Degradation of CMG100-AR Solar Cell Coverglass

Yu Chen[1], Taishi Endo[1], Minoru Iwata[1], Kazuhiro Toyoda[1],
Teppei Okumura[2], Masato Takahashi[2], Mengu Cho[1]

1，Laboratory of Spacecraft Environment Interaction Engineering,
Kyushu Institute of Technology, Kitakyushu, Fukuoka, 804-8550
2, Japan Aerospace Exploration Agency, 2-1-1 Sengen, Tsukuba, Ibaraki, 305-8505

Abstract: The CMG100-AR solar cell coverglasses suffered with simulating space environments, such as, thermal cycling, protons irradiation and electrons irradiation. Their dielectric constant, vacuum volume resistivity, total electron emission yield, and FTIR and UV-VIS-NIR spectrums are measured. The spectrum analysis considering to the color centers related to the change of material properties is discussed.

Key words: Solar cell coverglass, degradation, total electron emission yield, spectrum analysis

0 Introduction

The differential surface charging due to surface electron emission of space materials, results from potential differences on the surface of a spacecraft of a few volts to several thousands of volts, also considering to injecting particles' parameters, dielectric constant and vacuum resistivity. Although typical a lower potential difference, this type of charging is often more destructive because it leads to damaging surface discharge or arcing [1].

Cover glass is used to protect solar cells from damage, which would otherwise occur due to ultra-violet, electron and proton irradiation. Cover glasses are normally coated in order to transmit sunlight efficiently. Anti-Reflecting (AR) MgF_2 coating prevents reflecting sunlight. The change on material properties due to a long-term operation in space orbit should be studied and it will be helpful to understand the surface charging behavior of solar cell panel [2].

Kawakita et. al. [3] investigated the TEEY of CMG-100AR cover glasses with and without 1 MeV E-beam or 50 keV P-beam irradiation, and his results show the TEEY decreases with degradation, and he thought the displacement defects should be contributed to it, but he didn't clarify them in details. Miyage et. al. [4] studied the TEEY of CMG-100AR cover glasses with and without 500 keV E-beam or UV irradiation, and he obtained different experimental results with Kawakita. Nitta et. al. [5] studied the TEEY of atomic-oxygen-irradiated CMG-100AR cover glasses, and the results show the TEEY of AO irradiated coverglass decreased with increasing the AO fluence. They all used the TEEY measurement system with the range of 600~5000 eV in KEK. The yield test below 600 eV is not available due to its limitation.

In our previous work [6], we developed a TEEY measurement system with the range of 50~2500 eV, so we can obtain the full energy yield curves. In our project funded by JAXA, we are carrying out the single-factor degradation and multi-factors-in-series degradation induced by simulating space environments, such as, thermal cycling, electrons, protons, UV, and AO irradiations. Unfortunately, the joint-multi-factors degradation is not available in present situation in this project.

In this paper, we report the preliminary experimental results on material properties of four kinds of samples including of as-received, thermal cycles aged, proton beam irradiated, and electron beam irradiated samples. Their dielectric constant, vacuum volume resistivity, total electron emission yield, and FTIR and UV-VIS-NIR spectrums are obtained and the results are discussed.

1 Experimental preparation

1.1 Experimental samples

The specification of CMG100-AR coverglasses is listed in Table 1. It is widely used in most major satellite programs for both civilian and military applications.

Table 1: Specification of samples

Sample	CMG100-AR solar cell coverglass
Manufacture	Qioptiq Space Technology, UK
Front surface	110 nm thick MgF_2 coating
Substrate	100 μm thick CMG
Doping	Cerium doped
Substrate density	2.554 g/cm^3
Min. transmission	83.5%, 350 - 400 nm, 95.0%, 400 - 450 nm 97.0%, 450 - 900 nm, 96.5%, 900 - 1800 nm

1.2 Irradiating conditions

The irradiating conditions used in this research are listed in Table 2.

Table 2: Irradiated conditions

Type	Thermal cycling	P-beam	E-beam
Spec.	-160 °C ~ +110 °C	50 keV	500 keV
Fluence	348 cycles	7.8×10^{19} /m^2	1.4×10^{20} /m^2
Flux	-	6.14×10^{16} cm^{-2}s^{-1}, 1270 s	(1) 5.07×10^{14}cm^{-2}s^{-1}, 138100 s (2) 1.96×10^{16}cm^{-2}s^{-1}, 3580 s
Place	Laseine	Wakasa	Takasaki

1.3 Measured items

The measured material parameters are list in Table 3.

Table 3: Measured material parameters

Material property	Description
Dielectric frequency spectrum (DFS)	1 Hz ~ 1 MHz
Vacuum volume resistivity (VVR)	Polarization voltage: 500 V Max. Polarization time, 12 h
Total electron emission yield (TEEY)	Injecting energy: 50 ~ 2500 eV Primary electron beam current: ~ 50 nA
FTIR and UV-Vis-NIR spectrum	FTIR: 400 ~ 6000 cm^{-1} UV-Vis-NIR: 250 ~ 2500 nm

2 Simulating and experimental Results

2.1 Monte Carol simulations

(1) E-beam injecting simulation

Using Casino V2.42, the electron distribution with depth is simulated and plotted in Figure 1 while injecting with 500 keV electron beam. In the simulating model, iron (Fe) is used as substrate material. Beam landing spot radius is 10 nm, and the number of primary electrons is 100,000. With the energy of 500 keV, nearly there are no electrons that deposit in the coverglass, and the electron average range is 519 μm in SUS substrate.

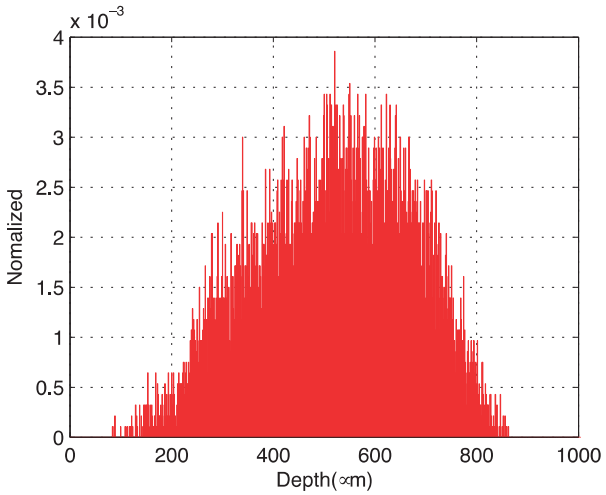

Figure 1: Electron distribution with depth

(2) P-beam injecting simulation

Using SRIM2011, the ion distribution with depth is simulated and plotted in Figure 2 while injecting with 50 keV proton beam. The weight density of AR coating (MgF_2) is 3.18 g/cm^3, and the weight density of coverglass is 2.554 g/cm^3. The number of primary ions is 99,999. Only 0.0475% ions deposit in the AR coating layer, all the other part deposit in the CMG substrate, and ion average range is 515 nm.

2.2 Dielectric frequency spectrum

At room temperature, the dielectric frequency spectrums of the four kinds of samples were measured by using Solartron SI 1260, and the results are shown in Figure 3 and Table 4. It can be found that the order of dielectric constants of four kinds of samples is 2 > 1 > 4 > 3 from 0.1 Hz to 1 MHz, and that is 4 > 2 > 1 > 3 from 0.01 Hz to 0.1 Hz.

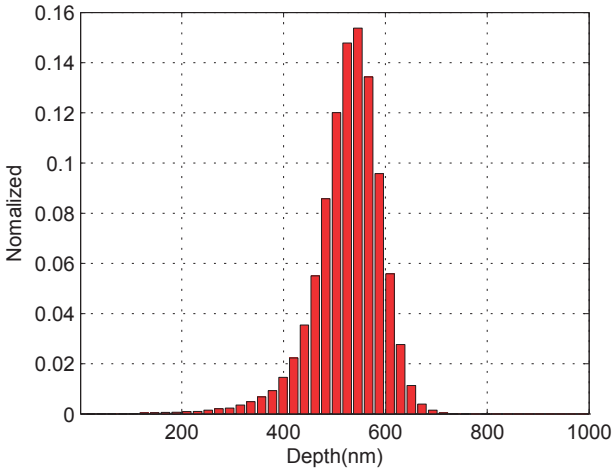

Figure 2: Ion distribution with depth

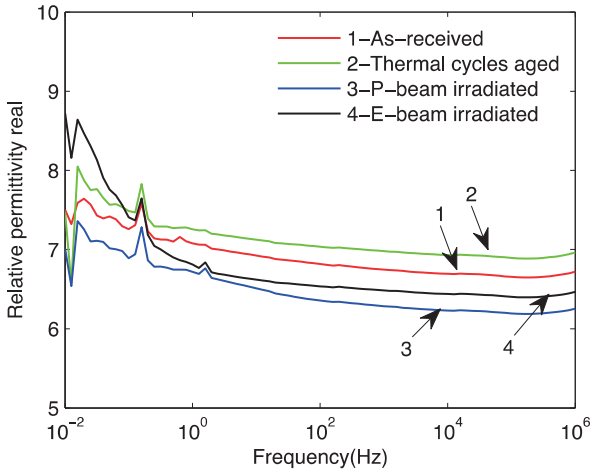

Figure 3: Dielectric frequency spectrum test by Solartron SI 1260.

Table 4: Dielectric constants of degraded coverglasses

f (Hz)	As-received	Thermal cycles aged	P-beam irradiated	E-beam irradiated
0.01	7.50	7.47	7.01	8.72
0.1	7.26	7.49	6.89	7.41
1	7.08	7.26	6.72	6.81
10	6.92	7.12	6.51	6.62
100	6.82	7.04	6.36	6.54
1000	6.75	6.98	6.28	6.49
10000	6.69	6.93	6.23	6.44
100000	6.66	6.89	6.19	6.40

2.3 Vacuum volume resistivity

The vacuum volume resistivity was measured by using the three electrodes recommended in ASTM D257. High voltage electrode was applied with 500 V powered by Keithly Model 6487 and the polarization current was also measured by it. The vacuum level is 7×10^{-5} Pa, and measuring time is up to 12 h. The results are shown in Figure 4, Figure 5, and Table 5. It can be found that the vacuum volume resistivity decreases due to degradation. From high to low, it follows the order of as-received, thermal cycles aged, e-beam irradiated, and p-beam irradiated samples.

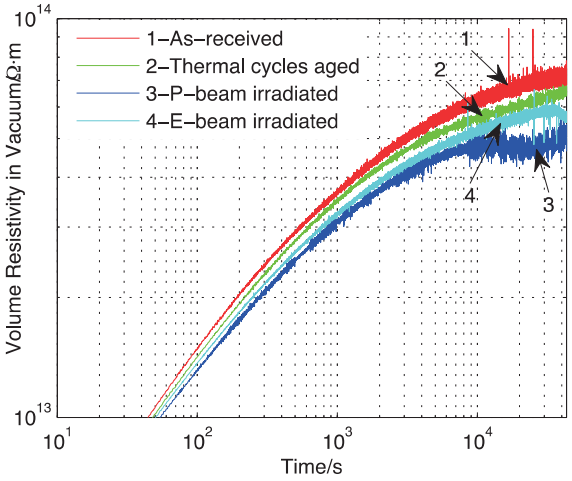

Figure 4: Volume resistivity in vacuum at room temperature

Table 5: Volume resistivity in vacuum at room temperature

Samples	*t* (min)	*I* (pA)	ρ_V ($\times10^{13}\Omega\cdot$m)
As-received	1	118.45	1.17
	30	31.67	4.36
	60	26.65	5.18
	720	19.24	7.18
Thermal cycles aged	1	124.23	1.11
	30	33.47	4.13
	60	28.61	4.82
	720	21.01	6.57
P-beam irradiated	1	131.65	1.05
	30	38.13	3.62
	60	32.79	4.21
	720	27.30	5.06
E-beam irradiated	1	127.25	1.08
	30	36.30	3.80
	60	31.12	4.44
	720	24.47	5.64

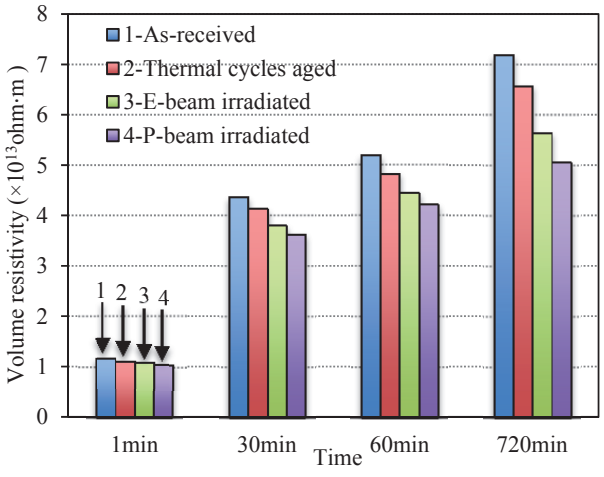

Figure 5: Volume resistivity in vacuum at 1 min, 30 min, 60 min and 720 min at room temperature

2.4 Total electron emission yield

We developed the TEEY measurement system, which can be referred to our previous work. By injecting a single pulse beam and using a small current detector for the total electron emission yield measurement of insulating material, the real charging-free TEEY $\sigma(E_P)$ as a function of the primary electron energy E_P can be measured. This system is developed based on JEOL JAMP-10 SXII Auger Microscope. Measurements were conducted in an ultra high vacuum system at a pressure of 7×10^{-5} Pa. The samples were metallized on the back-face with a 100 nm Au coating, cleaned using acetone in ultrasonic cleaner, and dried in heating oven for 24 h before introduction into the vacuum chamber. The electron beam current was ~50 nA on a spot area of ~1–1.5 mm^2 with a short duration time 50 μs. The results are shown in Figure 6.

It can be found that the TEEY decreases due to the material degradation. The TEEY of thermal cycles aged sample decrease slightly, the peak yield changes to 6.76 at 1000 eV. The P-beam irradiated sample shows the lowest TEEY, the peak yield is just 2.62, and the peak energy shifts to 600 eV. About the E-beam irradiated sample, its peak yield is 6.53 at the low energy of 400 eV.

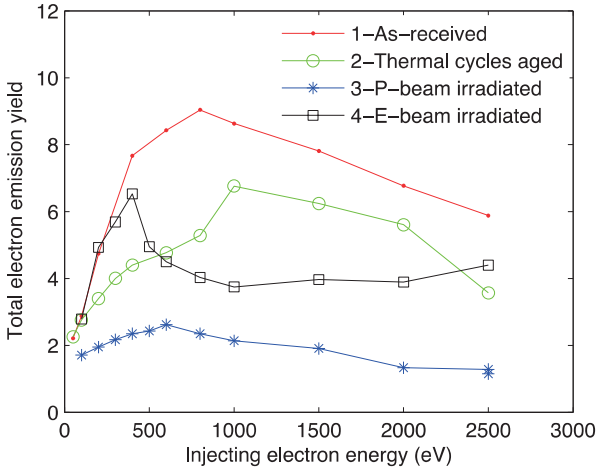

Figure 6: Total electron emission yield

2.5 FTIR and UV-VIS-NIR spectrum

(1) FTIR spectrum

The transmittance and reflectance FTIR spectrum were measured from 500 cm^{-1} to 2500 cm^{-1}, and the absorbance FTIR spectrum was calculated and shown in Figure 7. At 1060 cm^{-1}, the absorbance peak can be contributed to the stretching vibration of non-bridging silicone-oxygen bond (Si-O). The absorbance intensity of P-beam irradiated sample is highest at 1060 cm^{-1}, it means that the content of Si-O bond increases due to strong ionization effects by P-beam.

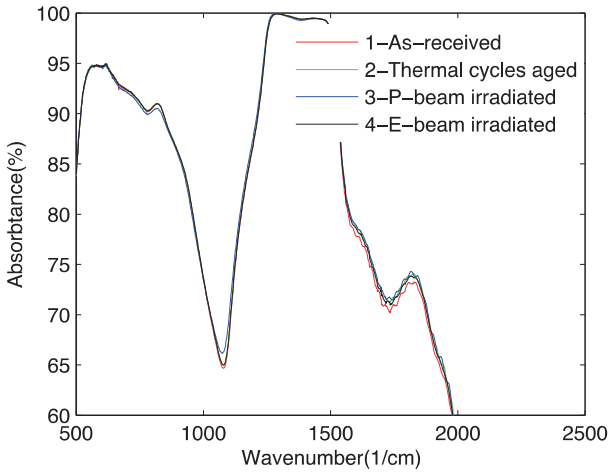

Figure 7: FTIR absorbance spectrum from 500 cm^{-1} to 2500 cm^{-1}

(2) UV-VIS-NIR spectrum

The typical color center and their defect structures of MgF_2 and SiO_2 are list in Table 6. The transmittance spectrum from 250 nm to 2500 nm was measured and shown in Figure 8(a), and the T_0-T spectrum was calculated and shown in Figure 8(b). For thermal cycles aged sample, the absorbance range is from 300 nm to 500 nm, for the other two samples, they are from 300 nm to 650 nm. The analysis results on the T_0-T spectrum using Gaussian fitting are listed in Table 7.

Table 6: Typical color center and their defect structures [7-11]

Material	Type	Color center	Wavelength (nm)
MgF_2	—Mg•	F	260
	—Mg• in gather	F_2	320
			370
			400
			437
SiO_2	=Si• •Si=	E’	213
	≡Si—Si≡	Oxygen-Deficient Center, ODC(1)	250
	=Si:	ODC(2)	460
	≡Al—O—Si≡	Aluminum impurity	550
	≡Si—O•	Non-bridging oxygen hole center	650

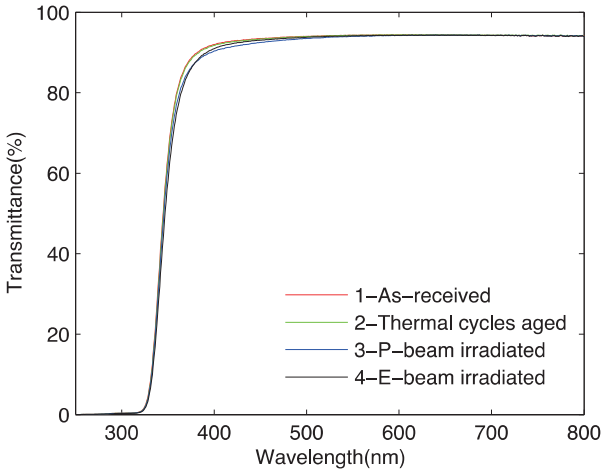

(a) Transmittance

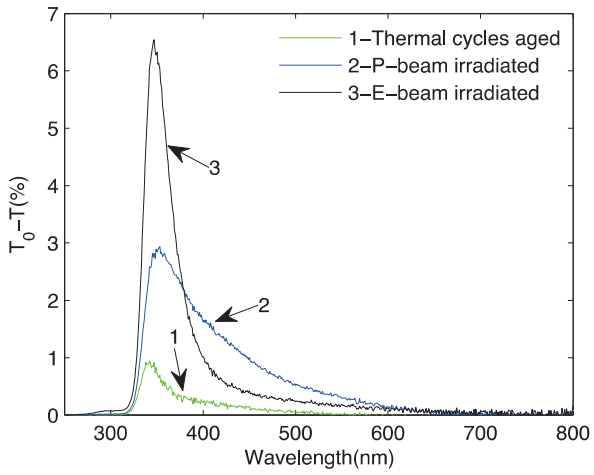

(b) T_0-T

Figure 8: UV-VIS-NIR Spectrum from 250 nm to 800 nm

Table 7: Analysis on the T_0-T spectrum using Gaussian fitting

Degradation type	Absorption peak position	Absorption peak intensity	Color center type
Thermal cycles aged	340	0.684	-
	359	0.319	MgF_2, F_2
	411	0.190	MgF_2, F_2
P-beam irradiated	350	1.319	-
	365	1.347	MgF_2, F_2
	340	1.069	-
	389	0.884	MgF_2, F_2
	423	0.742	MgF_2, F_2
	491	0.432	ODC(2)
E-beam irradiated	350	3.436	-
	364	2.021	MgF_2, F_2
	340	2.909	-
	384	0.712	MgF_2, F_2
	416	0.290	MgF_2, F_2
	510	0.148	ODC(2)

The results show that the F_2 center increases for three kinds of samples due to degradation, the ODC(2) increases by irradiating P-beam and E-beam.

3 Discussions

The electron beam can pass through the coverglass, the defects induced by it can form not only coating layer and also main substrate. The proton beam just can reach to ~500 nm deep from surface, in spite of small injecting distance, the number of generated defects is also significant due to the strong ionization effect of protons. The new silicon-oxygen bond and ODC(2) radical can decrease the permittivity and increase the volume resistivity. For TEEY, the secondary electron escaping depth is usually within several tens of nm, so it will be influenced by the M color center (F_2, F_3…) defects in MgF_2 layer. The M color center can capture the injecting electrons and reduce the emission probability.

4 Conclusions

(1) The permittivity increased due to degradation.

(2) The vacuum volume resistivity, TEEY, and transmittance of tested samples decreased due to degradation.

(3) The defects ODC(2) in CMG substrate of cover glasses due to degradation can be contributed to increasing on dielectric constant and decreasing on VVR.

(4) The defects, such as, F_2 center in MgF_2 coating layer due to degradation should be contributed to the decreasing on TEEY of tested samples.

ACKNOWLEDGEMENT

This work is supported by Japan Aerospace Exploration Agency.

REFERENCES

[1] Muranaka, T. Hosoda, S. Jeong-Ho Kim Hatta, S. Ikeda, K. Hamanaga, T. Cho, M. Usui, H. Ueda, H.O. Koga, K. Goka, T., Development of Multi-Utility Spacecraft Charging Analysis Tool (MUSCAT), IEEE Transactions on Plasma Science, 36(5),2008,pp: 2336–2349.

[2] Kumi Nitta, Eiji Miyazaki, Masato Takahashi, Current Status and Future Plan for Material Property Measurements Related to Engineering Design Optimization Guidelines and Spacecraft Charging at JAXA, ISMES, France, 2009.

[3] Kawakita, S. Imaizumi, M. Takahashi, M. Matsuda, S. Michizono, S. Saito, Y., Influence of High Energy Electrons and Protons on Secondary Electron Emission of Cover Glasses for Space Solar Cells, XXth ISDEIV, 2002.

[4] Hiroaki Miyake, Kumi Nitta, Shinichiro Michizono, and Yoshio Saito, Secondary Electron Emission on Degradation Sample and Development of New Measurement System with Low Electron Energy, XXIII-rd. Int. Symp. On Discharges and Electrical Insulation in Vacuum, Bucharest, 2008.

[5] Kumi Nitta, Chiharu Morioka, Eiji Miyazaki, Secondary Electron Emission Measurements of Atomic-Oxygen-Irradiated Cover glasses, 3rd AIAA Atmospheric Space Environments Conference, Honolulu, Hawaii, June 2011.

[6] Yu Chen, Takanori Kouno, Kazuhiro Toyoda, and Mengu Cho, Total electron emission yield measurement of insulator by a scanning small detector, Appl. Phys. Lett. 99, 152101, 2011.

[7] R. F. Blunt and M. I. Cohen, Irradiation-Induced Color Centers in Magnesium Fluoride, Phys. Rev. 153, 1031–1038 (1967)

[8] Christopher D. Marshall, Joel A. Speth, Stephen A. Payne, Induced optical absorption in gamma, neutron and ultraviolet irradiated fused quartz and silica, Journal of Non-Crystalline Solids, 212, 1997:59-73.

[9] H.-J. Fitting, A. N. Trukhin, T. Barfels, B. Schmidt, A. VON Czarnowski, Radiation induced defects in SiO2, Radiation Effects and Defects in Solids, 157:6-12, 2002, pp:575-581.

[10] W.A.Sibley and O.E.Facey, Color centers in MgF2, Physical Review, 174(3), 1968, pp:1076-1082.

[11] Sun Chengyue, An investigation on the space charged particle environmental effects of the coverglass for solar cell, Dissertation for Master Degree in Engineering, Harbin Institute of Technology, 2007.